Article

Not peer-reviewed version

Modelling Lifetime Data and Athletes Red Cells Counts Using the New Topp-Leone-Lomax Poisson Distribution

Mavis Pararai * and Fastel Chipepa *

Posted Date: 11 October 2024

doi: 10.20944/preprints202410.0885.v1

Keywords: Topp-Leone Lomax Distribution; Power Series Distribution; Maximum Likelihood Estimation; Poisson Distribution

Article

Modelling Lifetime Data and Athletes Red Cells Counts Using the New Topp-Leone-Lomax Poisson Distribution

Mavis Pararai [1,*] and Fastel Chipepa [2,*]

1 Department of Mathematical and Computer Sciences, Indiana University of Pennsylvania, Pennsylvania, USA
2 Department of Mathematics and Statistical Sciences, Botswana International University of Science and Technology, Palapye, Botswana
* Correspondence: pararaim@iup.edu (M.P.); chipepaf@biust.ac.bw (F.C.)

Abstract: A new compounded distribution called the Topp-Leone-Lomax Poisson is developed. The statistical properties of this model are derived. The model parameters are estimated via the maximum likelihood technique. The performance of the estimation techniques was assessed by means of simulation studies. The new model was exposed to three data sets and compared to other models within the same class and the evidence supports the importance of the new model in data modelling.

Keywords: Topp-Leone Lomax distribution; power series distribution; maximum likelihood estimation; poisson distribution

---

1. Introduction

Over the past two centuries, statistical distributions gained appreciation from many researchers as a means of describing data. A number of distributions were developed and these include the exponential distribution which was a very important lifetime distribution. This distribution was good in modelling lifetime data with constant failure rate. However, the distribution could not accommodate other failure rates that include decreasing, increasing and non-monotone. Lomax developed the shifted Pareto (Pareto II) or Lomax distribution [9] which is a mixture of the exponential and gamma distributions. This distribution applies to data with decreasing failure rate and has heavier tails compared to the Weibull [19] and gamma distributions. Statisticians came with solutions to address the short comings of classical distributions. These solutions include transformation of the classical distribution for example the T-X transformation by Alzaatreh et al. [4], gamma transformations by Zografos and Balakrishnan [20], Ristiç and Balakrishnan [15], and Torabi and Montazari [18], half logistic transformation by Cordeiro et al. [7], to mention a few. The other techniques for generalizing classical distribution includes exponentiation, power transformation, competing risks, and compounding methods.

Some generalizations of the Lomax distribution include the exponentiated Lomax (Exp-Lx) by Abdul-Moniem and Abdel-Hammed [2], exponential Lomax (E-Lx) by Bassiouny et al. [5], and the Weibull-Lomax (W-Lx) by Tahir et al. [17]. Oguntunde et al. [13] developed the Topp-Leone Lomax (TL-Lx) distribution using the generalization by Al-Shomrani et al. [3]. The TL-Lx distribution is a has a pdf that is skewed to the right. The TL-Lx distribution has cumulative distribution function (cdf) and probability density function (pdf) given by

$$G(x;\alpha,b,\lambda) = [1-(1+\lambda x)^{-2b}]^{\alpha} \tag{1}$$

and

$$g(x;\alpha,b,\lambda) = 2\alpha b\lambda(1+\lambda x)^{-(2b+1)}[1-(1+\lambda x)^{-2b}]^{\alpha-1}, \tag{2}$$

respectively, for $\alpha, b, \lambda > 0$. Other generalizations that involves the Topp-Leone generalization include the Topp-Leone odd exponential half logistic-G family of distributions by Chipepa and Oluyede [6], The Topp-Leone-Harris-G family of distributions with applications by Oluyede et al. [12], and the Topp-Leone odd Burr III-G family of distributions by Moakofi et al. [11].

This research generalizes the TL-LxP distribution by compounding it with the power series distribution. Power series distributions includes the Poisson, logarithmic, binomial, and geometric distributions as stated by Johnson et al. [8]. The Poisson distribution is considered as a special case from the power series distributions. Given a discrete random variable, say, M, having a power series distribution with probability mass function (pmf)

$$P(M=m)=\frac{a_m\theta^m}{C(\theta)}, m=1,2,..., \tag{3}$$

where $C(\theta)=\sum_{m=1}^{\infty}a_m\theta^m$ is finite, $\theta>0$ and $\{a_m\}_{m\geq 1}$ a sequence of positive real numbers. Taking $X_{(1)}=\min(X_1,X_2,...,X_M)$, the cumulative distribution function (cdf) and probability density function (pdf) of $X_{(1)}|M=m$ are defined by

$$F_{X_{(1)}|M=m}(x)=1-\frac{C(\theta S(x))}{C(\theta)}, \tag{4}$$

and

$$f_{X_{(1)}|M=m}(x)=\frac{\theta g(x)C'(\theta S(x))}{C(\theta)}, \tag{5}$$

where $S(x)$ is the survival function given by $1-F(x)$.

The rest of the paper is organized as follows: Statistical properties are presented in Section 2. Maximum likelihood estimation technique is presented in Section 3. Simulation study and inference are presented in Sections 4 and 5, followed by conclusion in Section 6.

2. The Model

In this paper, the TL-Lx distribution by Oguntunde et al. [13] is compounded with the Poisson power series distribution to produce a new model called the Topp-Leone-Lomax Poisson (TL-LxP) distribution. The pdf and the cdf of the TL-LxP distribution is given by

$$F(x;\alpha,b,\lambda,\theta)=1-\frac{\exp\left[\theta(1-[1-(1+\lambda x)^{-2b}]^{\alpha})\right]-1}{[\exp(\theta)-1]}, \tag{6}$$

and

$$\begin{aligned} f(x;\alpha,b,\lambda,\theta) &= \frac{2\alpha b\lambda\theta(1+\lambda x)^{-(2b+1)}[1-(1+\lambda x)^{-2b}]^{\alpha-1}}{\exp(\theta)-1} \\ &\times \exp\left[\theta(1-[1-(1+\lambda x)^{-2b}]^{\alpha})\right], \end{aligned} \tag{7}$$

for $\alpha,b,\lambda,\theta>0$. The corresponding hazard rate function is given by

$$\begin{aligned} h(x;\alpha,b,\lambda,\theta) &= \frac{2\alpha b\lambda\theta(1+\lambda x)^{-(2b+1)}[1-(1+\lambda x)^{-2b}]^{\alpha-1}}{\exp\left[\theta(1-[1-(1+\lambda x)^{-2b}]^{\alpha})\right]-1} \\ &\times \exp\left[\theta(1-[1-(1+\lambda x)^{-2b}]^{\alpha})\right]. \end{aligned} \tag{8}$$

The pdf of the TL-LxP takes reverse-J shape, right or left-skewed shapes as shown in Figure 1.

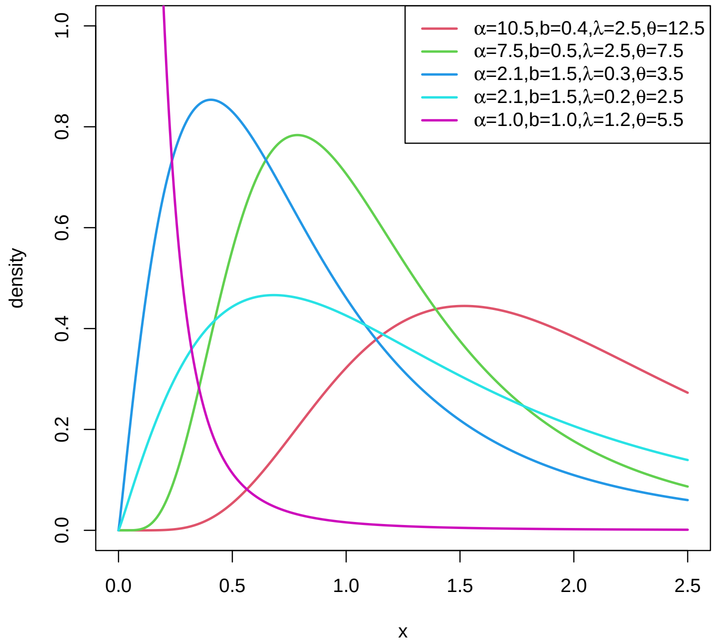

Figure 1. PDF Plots for TL-LxP Distribution.

3. Some Statistical Properties

We present in this section quantile function, moments, moment generation function, and Rényi Entropy.

3.1. Quantile Function

The u^{th} quantile function is defined by $F(x) = u, 0 < x < 1$. That is

$$1 - \frac{\exp\left[\theta(1 - [1 - (1 + \lambda x)^{-2b}]^{\alpha})\right] - 1}{[\exp(\theta) - 1]} = u$$

which simplifies to

$$x = \frac{1}{\lambda}\left\{\left[1 - \left\{\frac{\theta - \ln[1 + (1-u)(e^{\theta} - 1)]}{\theta}\right\}^{\frac{1}{\alpha}}\right]^{-\frac{1}{2b}} - 1\right\} \tag{9}$$

The first, second and third quantiles for the TL-LxP distribution are obtained by substituting in equation (9) $u = 0.25, 0.5$ and 0.75, respectively. Table 1 show quantile values for the TL-LxP distribution for selected parameter values ($\alpha, b, \lambda,$ and θ).

Preprints.org (www.preprints.org) | NOT PEER-REVIEWED | Posted: 11 October 2024 doi:10.20944/preprints202410.0885.v1

Table 1. Quantile values for selected parameter values.

u	(1.5,1.5,0.1,1.5)	(0.5,1,0.5,0.9)	(1.5,0.5,0.3,1.5)	(0.5,1.5,0.9,0.5)	(1.1,1.1,0.3,0.6)
0.1	0.5267	0.00461	0.5549	0.0024	0.1585
0.2	0.9252	0.0200	1.0134	0.0101	0.3278
0.3	1.3448	0.04923	1.5337	0.0244	0.5264
0.4	1.8225	0.0973	2.1748	0.0472	0.7693
0.5	2.3994	0.1731	3.0212	0.0818	1.0792
0.6	3.1417	0.2929	4.2321	0.1344	1.4967
0.7	4.1807	0.4918	6.1721	0.2176	2.1059
0.8	5.8442	0.8624	9.9251	0.3628	3.1224
0.9	9.3687	1.7807	20.8868	0.6879	5.3899

3.2. Moments and Moment Generating Function

The r^{th} raw moment (μ_r) of the TL-LxP distribution is given by

$$\mu_r = E(X^r) = \int_{-\infty}^{\infty} x^r f(x;\alpha,b,\lambda,\theta)dx, \tag{10}$$

with $f(x;\alpha,b,\lambda,\theta)$ defined in Equation (7). Using the generalized binomial series expansion $(1-z)^a = \sum_{j=0}^{\infty}(-1)^j\binom{a}{j}z^j$, we have

$$E(X^r) = \sum_{i,j=0}^{\infty}\binom{i}{j}\frac{(-1)^j 2\alpha b\lambda\theta^{i+1}}{(e^\theta-1)i!}\int_0^\infty x^r(1+\lambda x)^{-(2b+1)}[1-(1+\lambda x)^{-2b}]^{\alpha+j-1}dx.$$

Let $u = 1+\lambda x$, implying $x = \frac{1}{\lambda}(u-1)$ and $du = \lambda dx$, we get

$$\begin{aligned}\int_1^\infty x^r(1+\lambda x)^{-(2b+1)}[1-(1+\lambda x)^{-2b}]^{\alpha+j-1}dx &= \sum_{m=0}^{\infty}(-1)^m\binom{\alpha+j-1}{m} \\ &\times \int_1^\infty \frac{1}{\lambda^{r+1}}(u-1)^r u^{-2mb-2b-1}du.\end{aligned}$$

Thus,

$$\begin{aligned}\int_1^\infty \frac{1}{\lambda^{r+1}}(u-1)^r u^{-2mb-2b-1}du &= \int_0^\infty \frac{(u-1)^{(r+1)-1}}{\lambda^{r+1}u^{2mb+2b+1}}du \\ &= \frac{1}{\lambda^{r+1}}\int_0^\infty \frac{(u-1)^{(r+1)-1}}{u^{2mb+2b+1}}du \\ &= \frac{1}{\lambda^{r+1}}B(r+1,2mb+2b+1-(r+1)) \\ &= \frac{1}{\lambda^{r+1}}B(r+1,2mb+2b-r) \\ &= \frac{\Gamma(r+1)\Gamma(2mb+2b-r)}{\lambda^{r+1}\Gamma(2mb+2b+1)}\end{aligned}$$

which is a beta function over a half line. Therefore, the r^{th} moment is given by

$$E(X^r) = \sum_{i,j,m=0}^{\infty}\frac{(-1)^{j+m}2\alpha b\theta^{i+1}}{(e^\theta-1)i!\lambda^r}\binom{i}{j}\binom{\alpha+j-1}{m}\frac{\Gamma(r+1)\Gamma(2mb+2b-r)}{\lambda^{r+1}\Gamma(2mb+2b+1)}. \tag{11}$$

This result is important in determining the moments and measures of central tendency and dispersion (standard deviation (SD), coefficient of variation (CV), coefficient of skewness (CS), and coefficient of kurtosis (CK)). Table 2 presents the first five moments and the measures of dispersion for selected parameter values ($\alpha, b, \lambda,$ andθ).

Preprints.org (www.preprints.org) | NOT PEER-REVIEWED | Posted: 11 October 2024 doi:10.20944/preprints202410.0885.v1

Table 2. First five moments and measures of dispersion for selected parameter values.

	(1.5,1.5,0.1,1.5)	(0.5,1,0.5,0.9)	(1.1,0.5,0.8,1.5)	(1.5,1.5,0.9,0.5)	(1.1,0.9,0.3,0.6)
$E[X]$	0.1208	0.1736	0.2224	0.2903	0.1827
$E[X^2]$	0.0823	0.0873	0.1277	0.1540	0.1139
$E[X^3]$	0.0622	0.0569	0.0878	0.1002	0.0820
$E[X^4]$	0.0498	0.0419	0.0664	0.0730	0.0638
$E[X^5]$	0.0415	0.0331	0.0532	0.0570	0.0521
SD	0.2603	0.2390	0.2797	0.2641	0.2838
CV	2.1555	1.3770	1.2579	0.9096	1.5535
CS	2.0333	1.6097	1.1231	0.8146	1.3891
CK	5.7439	4.7457	3.0822	2.7208	3.6022

The moment generating function of the TL-LxP is given by

$$\begin{aligned} M_X(t) = E[e^{tX}] &= \sum_{p=0}^{\infty} \frac{t^p E[X^p]}{p!} \\ &= \sum_{i,j,m,p=0} \frac{(-1)^{j+m} 2\alpha b \theta^{i+1}}{(e^\theta - 1) i! p! \lambda^p} \binom{i}{j} \binom{\alpha + j - 1}{m} \frac{\Gamma(p+1)\Gamma(2mb + 2b - p)}{\lambda^{p+1}\Gamma(2mb + 2b + 1)} \end{aligned} \tag{12}$$

3.3. Distribution of Order Statistics

The pdf of the i^{th} order statistics is given by

$$\begin{aligned} f_{i:n}(x) &= \frac{n! f(x)}{(i-1)!(n-i)!} \sum_{q=0}^{\infty} (-1)^q \binom{n-1}{q} [F(x)]^{q+i-1} \\ &= \frac{n! 2\alpha b \lambda \theta (1 + \lambda x)^{-(2b+1)}}{(i-1)!(n-i)!(e^\theta - 1)} [1 - (1+\lambda x)^{-2b}]^{\alpha - 1} \exp[\theta(1 - [1 - (1+\lambda x)^{-2b}]^\alpha)] \\ &\times \sum_{q=0}^{\infty} (-1)^q \binom{n-1}{q} \left\{ 1 - \frac{\exp[\theta(1 - [1 - (1+\lambda x)^{-2b}]^\alpha)] - 1}{e^\theta - 1} \right\}^{q+i-1} \\ &= \frac{n! 2\alpha b \lambda \theta}{(i-1)!(n-i)!} \sum_{q,s,t=0}^{\infty} \frac{(-1)^{q+s+t}(1+t)}{(1+t)(e^\theta - 1)^{s+1}} \binom{n-1}{q} \binom{q+i-1}{s} \binom{s}{t} (1+\lambda x)^{-(2b+1)} \\ &\times [1 - (1+\lambda x)^{-2b}]^{\alpha - 1} \exp[\theta(1+t)(1 - [1 - (1+\lambda x)^{-2b}]^\alpha)] \end{aligned} \tag{13}$$

which is a linear combination of exponentiated TL-Lx distribution.

3.4. Rényi Entropy

The two commonly used measures of uncertainty are Shannon [16] and Rényi [14] entropies. Rényi entropy is a generalization of the Shannon entropy, hence, we will derive only the Rényi entropy in this paper. Rényi entropy for the TL-LxP distribution is derived as follows:

$$I_R(\nu) = \frac{1}{1-\nu} \log \left(\int_0^\infty [f(x;\alpha, b, \lambda, \theta)]^\nu dx \right). \tag{14}$$

$$\begin{aligned} [f(x;\alpha, b, \lambda, \theta)]^\nu &= \left[\frac{2\alpha b \lambda \theta}{e^\theta - 1} \right]^\nu (1+\lambda x)^{-(2b\nu + \nu)} [1 - (1+\lambda x)^{-2b}]^{\alpha\nu - \nu} \\ &\times \exp[\theta\nu(1 - [1 - (1+\lambda x)^{-2b}]^\alpha)] \\ &= \left[\frac{2\alpha b \lambda \theta}{e^\theta - 1} \right]^\nu \sum_{t,s,u=0}^{\infty} \frac{(-1)^{t+u}(\theta\nu)^s}{s!} \binom{s}{t} \binom{\alpha t + \alpha\nu - \nu}{u} (1+\lambda x)^{-2bu - 2b\nu - \nu}. \end{aligned}$$

 doi:10.20944/preprints202410.0885.v1

Now

$$\int_0^\infty (1+\lambda x)^{-2bu-2bv-v} dx = \int_0^\infty \frac{dx}{(1+\lambda x)^{2bu+2bv+v}}.$$

Let $u = 1+\lambda x \implies du = \lambda dx \implies dx = \frac{1}{\lambda} du$. When $x = 0, \; u = 1$ and when $x = \infty, \; u = \infty$. Note

$$\int_1^\infty \frac{(t-1)^a}{t^b} = B(a+1, b-a-1) = \frac{\Gamma(a+1)\Gamma(b-a-1)}{\Gamma(b)}.$$

Hence,

$$\begin{aligned} \int_1^\infty \frac{dx}{(1+\lambda x)^{2bu+2bv+v}} &= \frac{1}{\lambda}\int_1^\infty \frac{(u-1)^{1-1}}{(1+\lambda x)^{2bu+2bv+v}} \\ &= \frac{1}{\lambda}\frac{\Gamma(1)\Gamma 2bu+2bv+v-1}{\Gamma(2bu+2bv+v)} \\ &= \frac{1}{\lambda(2bu+2bv+nu-1)}. \end{aligned}$$

Therefore, we define Rényi entropy of the TL-LxP distribution by

$$I_R(v) = \frac{1}{1-v}\log\left[\left[\frac{2\alpha b\lambda\theta}{e^\theta - 1}\right]^v \sum_{t,s,u=0}^{\infty} \frac{(-1)^{t+u}(\theta v)^s}{s!}\binom{s}{t}\binom{\alpha t + \alpha v - v}{u}\frac{1}{\lambda(2bu+2bv+nu-1)}\right]. \tag{15}$$

4. Estimation

If $X_i \sim TL-LxP(\alpha, b, \lambda, \theta)$ with the parameter vector $\Delta = (\alpha, b, \lambda, \theta)^T$. The total log-likelihood $\ell = \ell(\Delta)$ from a random sample of size n is given by

$$\begin{aligned} \ell &= n\ln[2\alpha b\lambda\theta] - (2b+1)\sum_{i=1}^n \ln[1+\lambda x] + (\alpha-1)\sum_{i=1}^n \ln[1-(1+\lambda x)^{-2b}] \\ &+ \sum_{i=1}^n \theta[1-(1-[1+\lambda x]^{-2b})^\alpha] - \sum_{i=1}^n (e^\theta - 1). \end{aligned}$$

The elements of the score vector $U = \left(\frac{\partial \ell}{\partial \alpha}, \frac{\partial \ell}{\partial b}, \frac{\partial \ell}{\partial \lambda}, \frac{\partial \ell}{\partial \theta}\right)$ are given below

$$\frac{\partial \ell}{\partial \alpha} = \frac{n}{\alpha} + \sum_{i=1}^n \ln[1-(1+\lambda x)^{-2b}] - \sum_{i=1}^n \theta[1-(1+\lambda x)^{-2b}]^\alpha \ln[1-(1+\lambda x)^{-2b}],$$

$$\begin{aligned} \frac{\partial \ell}{\partial b} &= \frac{n}{b} - 2\sum_{i=1}^n \ln[1+\lambda x] + 2(\alpha-1)\sum_{i=1}^n \frac{\ln[1+\lambda x](1+\lambda x)^{-2b}}{1-(1+\lambda x)^{-2b}} \\ &- 2\sum_{i=1}^n \theta\alpha\ln[1+\lambda x](1+\lambda x)^{-2b}[1-(1+\lambda x)^{-2b}]^{\alpha-1}, \end{aligned}$$

$$\begin{aligned} \frac{\partial \ell}{\partial \lambda} &= \frac{n}{\lambda} - (2b+1)\sum_{i=1}^n \frac{\lambda}{1+\lambda x} + 2(\alpha-1)\sum_{i=1}^n \frac{bx(1+\lambda x)^{-2b-1}}{1-(1+\lambda x)^{-2b}} \\ &- 2\sum_{i=1}^n \theta b\alpha x(1+\lambda x)^{-2b}(1-[1+\lambda x]^{-2b})^{\alpha-1}, \end{aligned}$$

. and

Preprints.org (www.preprints.org) | NOT PEER-REVIEWED | Posted: 11 October 2024 doi:10.20944/preprints202410.0885.v1

$$\frac{\partial \ell}{\partial \theta} = \frac{n}{\theta} + \sum_{i=1}^{n} 1 - [1 - (1 + \lambda x)^{-2b}]^{\alpha} - n,$$

respectively. The solutions to the nonlinear equation $\left(\frac{\partial \ell}{\partial \alpha}, \frac{\partial \ell}{\partial b}, \frac{\partial \ell}{\partial \lambda}, \frac{\partial \ell}{\partial \theta}\right)^{T} = \mathbf{0}$, gives the maximum likelihood estimates of the model parameters.

5. Simulations

To evaluate the consistency of the model parameter estimation technique. A Monte Carlo simulation study was conducted. Results for the simulation study are summarised in Table 3. A simulation study was conducted for sample sizes n= 20, 40, 60,120, 240 and 480 for N=3000 repetitions from the TLL-LxP distribution. The average bias (AB) and root mean square error (RMSE) for an estimated parameter, say ($\hat{\Phi}$), is calculated using the following formulae

$$ABIAS(\hat{\Phi}) = \frac{\sum_{i=1}^{N} \hat{\Phi}_i}{N} - \Phi, \quad \text{and} \quad RMSE(\hat{\Phi}) = \sqrt{\frac{\sum_{i=1}^{N} (\hat{\Phi}_i - \Phi)^2}{N}},$$

respectively. The simulation study results demonstrates that the parameter estimates from the TL-LxP distribution are consistent since the mean values approaches the true parameter values for increasing sample size. Furthermore, RMSE and ABias decays as the sample size increases demonstrating consistence in the parameter estimation process. The results are presented in Table 3.

Preprints.org (www.preprints.org) | NOT PEER-REVIEWED | Posted: 11 October 2024 doi:10.20944/preprints202410.0885.v1

Table 3. Monte Carlo Simulation Results for the TL-LxP Distribution: Mean, RMSE and AB.

		(1, 1, 0.4, 1)			(1.0, 1.1, 0.4, 1.1)		
	n	Mean	RMSE	Bias	Mean	RMSE	Bias
	40	1.1187	0.4721	0.1187	1.1094	0.3637	0.1094
	80	1.0418	0.2124	0.0418	1.0438	0.2134	0.0438
α	100	1.0287	0.1808	0.0287	1.0268	0.1863	0.0268
	200	1.0141	0.1252	0.0141	1.0101	0.1200	0.0101
	400	1.0003	0.0886	0.0003	1.0008	0.0886	0.0008
	40	3.0728	4.6544	2.0728	3.4046	5.1203	2.3046
	80	2.1885	3.0581	1.1885	2.5260	3.6024	1.4260
b	100	1.8541	2.4040	0.8541	2.2194	2.9517	1.1194
	200	1.3472	1.2323	0.3472	1.6549	1.8163	0.5549
	400	1.1522	0.5702	0.1522	1.3192	0.7852	0.2192
	40	0.5926	3.1108	0.1926	0.4847	0.6640	0.0847
	80	0.3932	0.3985	-0.0068	0.4118	0.4269	0.0118
λ	100	0.3985	0.3761	-0.0015	0.4036	0.4167	0.0036
	200	0.3823	0.2763	-0.0177	0.3832	0.2979	-0.0168
	400	0.3670	0.2154	-0.0330	0.3746	0.2305	-0.0254
	40	1.7883	1.3726	0.7883	1.8600	1.3326	0.7600
	80	1.6869	1.2467	0.6869	1.7232	1.2241	0.6232
θ	100	1.6333	1.1739	0.6333	1.7066	1.1771	0.6066
	200	1.5767	1.1279	0.5767	1.6617	1.1304	0.5617
	400	1.4849	1.0079	0.4849	1.5532	1.0065	0.4532
		(1, 1.1, 0.4, 0.9)			(1.0, 1,0, 1.1, 1.1)		
	n	Mean	RMSE	Bias	Mean	RMSE	Bias
	40	1.1179	0.4445	0.1179	1.1161	0.4619	0.1161
	80	1.0481	0.2139	0.0481	1.0401	0.2156	0.0401
α	100	1.0297	0.1878	0.0297	1.0280	0.1891	0.0280
	200	1.0156	0.1221	0.0156	1.0100	0.1204	0.0100
	400	1.0010	0.0878	0.0010	1.0014	0.0876	0.0014
	40	3.3695	4.9285	2.2695	4.7556	8.7554	3.7556
	80	2.4850	3.3800	1.3850	3.3262	6.3080	2.3262
b	100	2.2942	2.9945	1.1942	2.5351	4.6243	1.5351
	200	1.6291	1.6175	0.5291	1.4946	2.0599	0.4946
	400	1.3773	0.8805	0.2773	1.1591	0.7450	0.1591
	40	0.4667	0.7443	0.0667	2.2409	19.8829	1.1409
	80	0.3895	0.4034	-0.0105	1.0952	1.1146	-0.0048
λ	100	0.3831	0.3863	-0.0169	1.1261	1.1634	0.0261
	200	0.3640	0.2778	-0.0360	1.0627	0.7570	-0.0373
	400	0.3461	0.2167	-0.0539	1.0402	0.6162	-0.0598
	40	1.7507	1.3448	0.8507	1.9460	1.7794	0.8460
	80	1.6485	1.2425	0.7485	1.8051	1.3196	0.7051
θ	100	1.5747	1.1319	0.6747	1.7437	1.2722	0.6437
	200	1.5370	1.0988	0.6370	1.6684	1.1725	0.5684
	400	1.4525	0.9974	0.5525	1.5819	1.1029	0.4819

 doi:10.20944/preprints202410.0885.v1

6. Inference

To assess the utility of the new compounded model. Three real data sets are used for demonstration purposes. The TL-LxP distribution was compared to the TL-Lx by Oguntunde et al. [13], exponentiated Lomax (Exp-Lx) by Abdul-Moniem and Abdel-Hammed [2], exponential Lomax (E-Lx) by Bassiouny et al. [5], and the Weibull-Lomax (W-Lx) by Tahir et al. [17]. Various goodness-of-fit (GoF) statistics were used to assess model performance. The GoF statistics used are the -2log-likelihood statistic $(-2\ln(L))$, Akaike Information Criterion (AIC), Bayesian Information Criterion (BIC) and Consistent Akaike Information Criterion (AICC), Cramér-von Mises (W^*) and Anderson-Darling (A^*). Generally, a good fitting model is expect to have smaller values for all the GoF statistics. Graphical displays were further used to demonstrate how the proposed model fit the data sets. The graphs considered are the histogram of data and fitted pdf, probability plot, fitted cdf, Kaplan-Meier curves, scaled total time on test (TTT) transform proposed by Aarset [1] and the fitted hazard rate function. Data analysis results are presented in Tables 4 and 5

6.1. Failure Times Data

The first dataset represents time to failure of 59 test conductors of 400 micrometer length. The specimens were subjected to high temperature and current density. The times to failure in hours for the 59 test conductors are shown below. 6.545, 9.289, 7.543, 6.956, 6.492, 5.459, 8.120, 4.706, 8.687,2.997, 8.591, 6.129, 11.038, 5.381, 6.958, 4.288, 6.522, 4.137, 7.459, 7.495, 6.573, 6.538, 5.589, 6.087, 5.807, 6.725, 8.532, 9.663,6.369, 7.024, 8.336, 9.218, 7.945, 6.869, 6.352, 4.700, 6.948, 9.254, 5.009, 7.489, 7.398, 6.033, 10.092, 7.496, 4.531, 7.974, 8.799, 7.683, 7.224, 7.365, 6.923, 5.640, 5.434, 7.937, 6.515, 6.476, 6.071, 10.491, 5.923.

Table 4 shows the model parameters and GoF statistics for the new model and some selected competing models. The standard errors for the parameter estimates are given in parenthesis. The estimated variance-covariance matrix for the TL-LxP model on the failure times dataset is given by

$$\begin{pmatrix} 2.5478 & 1.7123 & -0.0118 & 0.3297 \\ 1.7123 & 1.1507 & -0.0079 & 0.2216 \\ -0.0118 & -0.0079 & 5.5589\times10^{-5} & -0.0015 \\ 0.3297 & 0.2216 & -0.0015 & 0.0426 \end{pmatrix}$$

with the approximate asymptotic 95% two-sided confidence intervals for the parameter estimates α, b, λ and θ given by 10.6068 ± 3.1286, 3.2757 ± 2.1026, 0.0291 ± 0.0146 and 30.7911 ± 0.4049, respectively.

Table 4. Parameter Estimates and Goodness-of-Fit Statistics for Failure Times Data.

	Estimates				Statistics					
Model	α	b	λ	θ	$-2\log Ł$	AIC	$AICC$	BIC	W^*	A^*
TL-LxP	10.6068	3.2757	0.0291	30.7911	222.65	230.65	231.40	238.96	0.0354	0.2003
	(1.5962)	(1.0727)	(0.0075)	(0.2066)						
TL-Lx	53.9590	154.2200	0.0021	-	230.05	236.05	236.49	242.28	0.1061	0.6512
	(6.9886×10^{-10})	(9.9495×10^{-10})	(7.2301×10^{-5})	-						
Exp-Lx	53.2240	-	0.0015	424.1200	230.01	236.01	236.44	242.24	0.1053	0.6467
	(3.7181×10^{-10})	-	(5.2423×10^{-5})	(1.8960×10^{-10})						
E-Lx	101.2300	155.7100	0.0071	-	234.90	240.90	241.34	247.13	0.2237	1.2920
	(3.5910×10^{-7})	(2.2705×10^{-7})	(0.0009)	-						
	α	a	b	-						
W-Lx	9.5584	0.2642	1.6864	-	224.02	230.02	230.46	236.28	0.0669	0.3739
	(9.7424)	(0.3376)	6.0967	-						

The results presented in Table 4 shows that the TL-LxP distribution performs better than the other selected generalizations of the Lomax distribution available in the literature. This is supported by the evidence that the TL-LxP distribution has lower values for all the GoF statistics compared to the selected competing models. Graphical plots from the fitted model also show how good the TL-LxP distribution performs on the failure times dataset.

6.2. Red Cells Data

The second dataset represents red cell counts of 202 athletes from Australia. The data are was obtained from the sn package of the R software. The observations are as follows: 3.80, 3.90, 3.90, 3.91, 3.95, 3.95, 3.96, 3.96, 4.00, 4.02, 4.03, 4.06, 4.07, 4.08, 4.09, 4.09, 4.10, 4.11, 4.11, 4.12, 4.13, 4.13, 4.14, 4.15, 4.16, 4.16, 4.17, 4.17, 4.19, 4.20, 4.20, 4.21, 4.23, 4.23, 4.24, 4.24, 4.25, 4.26, 4.26, 4.27, 4.27, 4.30, 4.31, 4.31, 4.32, 4.32, 4.32, 4.35, 4.36, 4.36, 4.37, 4.38, 4.38, 4.39, 4.40, 4.40, 4.40, 4.41, 4.41, 4.41, 4.42, 4.42, 4.44, 4.44, 4.44, 4.45, 4.45, 4.46, 4.46, 4.46, 4.46, 4.46, 4.48, 4.49, 4.50, 4.50, 4.51, 4.51, 4.51, 4.51, 4.52, 4.53, 4.54, 4.55, 4.56, 4.57, 4.58, 4.62, 4.63, 4.63, 4.63, 4.64, 4.66, 4.68, 4.71, 4.71, 4.71, 4.71, 4.73, 4.75, 4.75, 4.76, 4.77, 4.77, 4.78, 4.81, 4.81, 4.82, 4.82, 4.83, 4.83, 4.83, 4.83, 4.84, 4.86, 4.86, 4.87, 4.87, 4.87, 4.87, 4.87, 4.87, 4.88, 4.89, 4.89, 4.90, 4.90, 4.91, 4.91, 4.92, 4.93, 4.93, 4.94, 4.95, 4.95, 4.96, 4.97, 4.97, 4.98, 4.99, 5.00, 5.00, 5.00, 5.01, 5.01, 5.01, 5.02, 5.02, 5.03, 5.03, 5.03, 5.03, 5.04, 5.04, 5.08, 5.09, 5.09, 5.09, 5.10, 5.11, 5.11, 5.11, 5.11, 5.11, 5.13, 5.13, 5.13, 5.13, 5.16, 5.16, 5.16, 5.16, 5.17, 5.17, 5.18, 5.21, 5.21, 5.22, 5.22, 5.24, 5.24, 5.25, 5.29, 5.31, 5.32, 5.33, 5.33, 5.34, 5.34, 5.34, 5.34, 5.38, 5.40, 5.48, 5.48, 5.49, 5.50, 5.59, 5.66, 5.69, 5.93, 6.72.

Table 5. Parameter Estimates and Goodness-of-Fit Statistics for Red Cells Data.

	Estimates				Statistics					
Model	α	b	λ	θ	$-2\log Ł$	AIC	$AICC$	BIC	W^*	A^*
TL-LxP	275.1900	18.0300	0.0287	12.1300	252.25	260.25	260.45	273.48	0.2756	1.4905
	(4.6929×10^{-9})	(3.2923×10^{-7})	(1.9392×10^{-4})	(3.9722×10^{-8})						
TL-Lx	2.3999×10^{4}	7.0413×10^{3}	1.5861×10^{-4}	-	262.89	268.89	269.01	278.82	0.4186	2.3022
	(7.6362×10^{-16})	(2.5623×10^{-14})	(1.1394×10^{-6})	-						
Exp-Lx	2.7839×10^{4}	-	3.6145×10^{-4}	6.2847×10^{3}	261.95	267.95	268.07	277.87	0.422	2.3240
	(3.3390×10^{-15})	-	(2.5735×10^{-6})	(1.4804×10^{-13})						
E-Lx	79.4110	46.9440	3.7495×10^{-4}	-	343.91	349.91	359.71	353.81	0.2664	2.1860
	(1.0190×10^{-9})	(1.6366×10^{-9})	(2.6382×10^{-5})	-						
	α	a	b	-						
W-Lx	14.1610	0.4390	0.7813	-	293.41	299.41	299.54	309.34	0.2224	1.8017
	(1.1162)	(0.0465)	(0.1648)	-						

It can be observed from the results shwon in Table 5 that the TL-LxP distribution performs better on red cell counts data compared to the other selected models since it has the smallest values for the goodness-of-fit statistics.

The estimated variance-covariance matrix for the TL-LxP model for Red cells dataset is given by

$$\begin{pmatrix} 2.2023\times10^{-17} & -1.5450\times10^{-15} & -9.1006\times10^{-13} & -1.8641\times10^{-16} \\ -1.5450\times10^{-15} & 1.0839\times10^{-13} & 6.3844\times10^{-11} & 1.3077\times10^{-14} \\ -9.1006\times10^{-13} & 6.3844\times10^{-11} & 3.7606\times10^{-8} & 7.7029\times10^{-12} \\ -1.8641\times10^{-16} & 1.3077\times10^{-14} & 7.7029\times10^{-12} & 1.5778\times10^{-15} \end{pmatrix}$$

and the approximate 95% two-sided confidence intervals for the parameter estimates are α, b, λ and θ are given by $275.1900 \pm 9.1981\times10^{-9}$, $18.0300 \pm 6.4529\times10^{-7}$, $0.0287 \pm 3.8009\times10^{-4}$ and $12.1300 \pm 7.7855\times10^{-8}$, respectively.

Preprints.org (www.preprints.org) | NOT PEER-REVIEWED | Posted: 11 October 2024 doi:10.20944/preprints202410.0885.v1

6.3. Acute Bone Cancer Data

The third dataset represents the survival times (in days) of 73 patients diagnosed with acute bone cancer as reported by Mansour et al. [10]. The data are as follows: 0.09, 0.76, 1.81, 1.10, 3.72, 0.72, 2.49, 1.00, 0.53, 0.66, 31.61, 0.60, 0.20, 1.61, 1.88, 0.70, 1.36, 0.43, 3.16, 1.57, 4.93, 11.07, 1.63, 1.39, 4.54, 3.12, 86.01, 1.92, 0.92, 4.04, 1.16, 2.26, 0.20, 0.94, 1.82, 3.99, 1.46, 2.75, 1.38, 2.76, 1.86, 2.68, 1.76, 0.67, 1.29, 1.56, 2.83, 0.71, 1.48, 2.41, 0.66, 0.65, 2.36, 1.29, 13.75, 0.67, 3.70, 0.76, 3.63, 0.68, 2.65, 0.95, 2.30, 2.57, 0.61, 3.93, 1.56, 1.29, 9.94, 1.67, 1.42, 4.18, 1.37.

Furthermore, results presented in Table 6 supports the superiority of the TL-LxP distribution compared to the other selected models. From the plots of the fitted densities (Figures 2, 5 and 8), we observe that the model is applicable to data containing some outlying values and that the model is applicable to data with increasing or non monotonic failure rates as shown in Figures 4, 7 and 10.

Table 6. Parameter Estimates and Goodness-of-Fit Statistics for Acute Bone Cancer Data.

	Estimates				Statistics					
Model	α	b	λ	θ	$-2\log Ł$	AIC	$AICC$	BIC	W^*	A^*
TL-LxP	2.5917	0.5558	0.5351	4.1833	278.29	286.29	286.88	295.45	0.0568	0.4391
	(0.7412)	(0.3128)	(0.4295)	(2.0482)						
TL-Lx	3.3768	0.9318	0.9169	-	281.67	287.67	288.02	294.54	0.0919	0.6886
	(1.1532)	(0.2168)	(0.9169)	-						
Exp-Lx	3.3768	-	0.9169	1.8637	281.67	287.67	288.02	294.54	0.0919	0.6886
	(1.1532)	-	(0.5215)	(0.4337)						
E-Lx	0.7659	2.6643×10^{-5}	1.3793×10^{-4}	-	322.81	328.81	329.15	335.68	0.6017	3.6470
	(9.2412×10^{-6})	(3.3325×10^{-4})	(1.3220×10^{-3})	-						
	α	a	b	-						
W-Lx	1.7750	0.2582	5.0702	-	300.52	306.52	306.87	313.87	0.3067	1.9958
	(0.4286)	(0.0759)	(4.3144)	-						

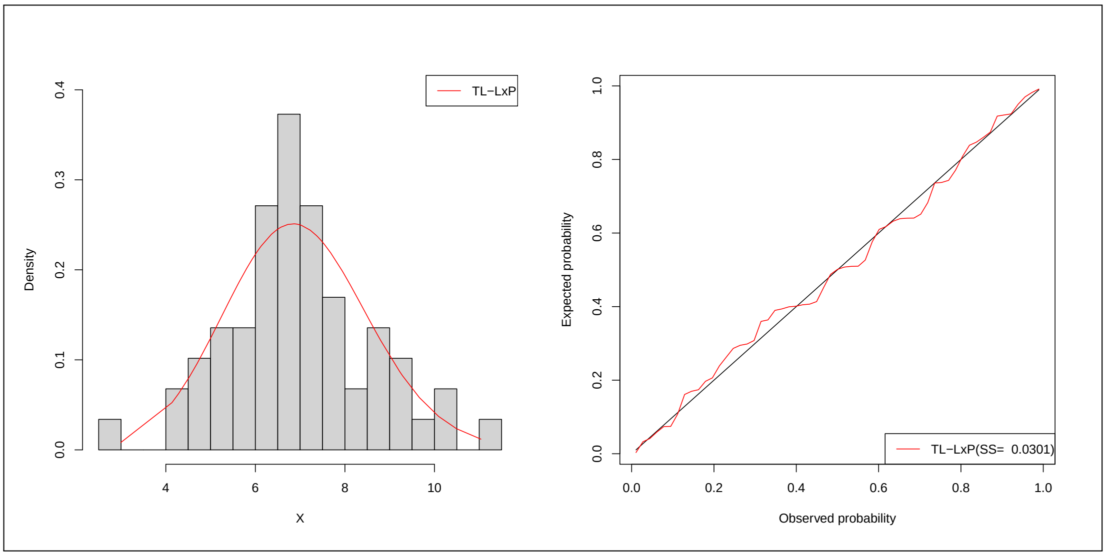

Figure 2. Fitted Densities and Probability Plots for Failure Times Data.

 doi:10.20944/preprints202410.0885.v1

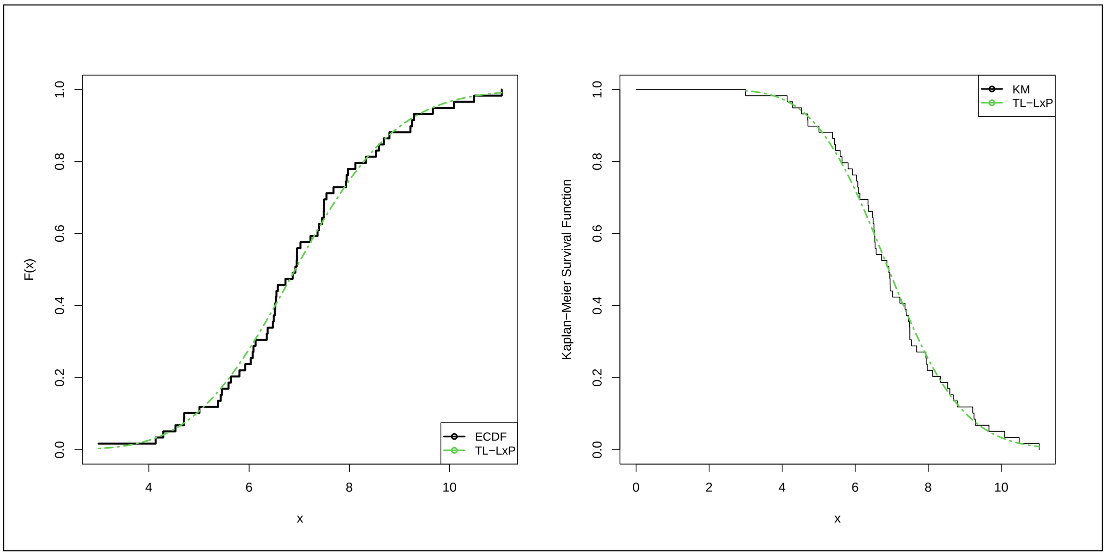

Figure 3. Fitted K-M and ECDF Plots for Failure Times Data.

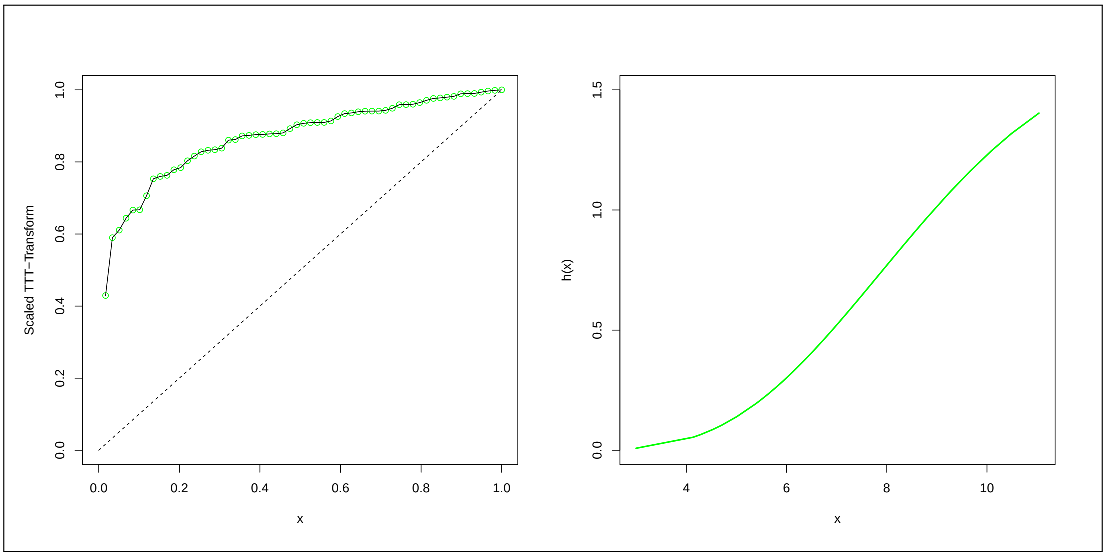

Figure 4. Fitted TTT and HRF Plots for Failure Times Data.

Preprints.org (www.preprints.org) | NOT PEER-REVIEWED | Posted: 11 October 2024 doi:10.20944/preprints202410.0885.v1

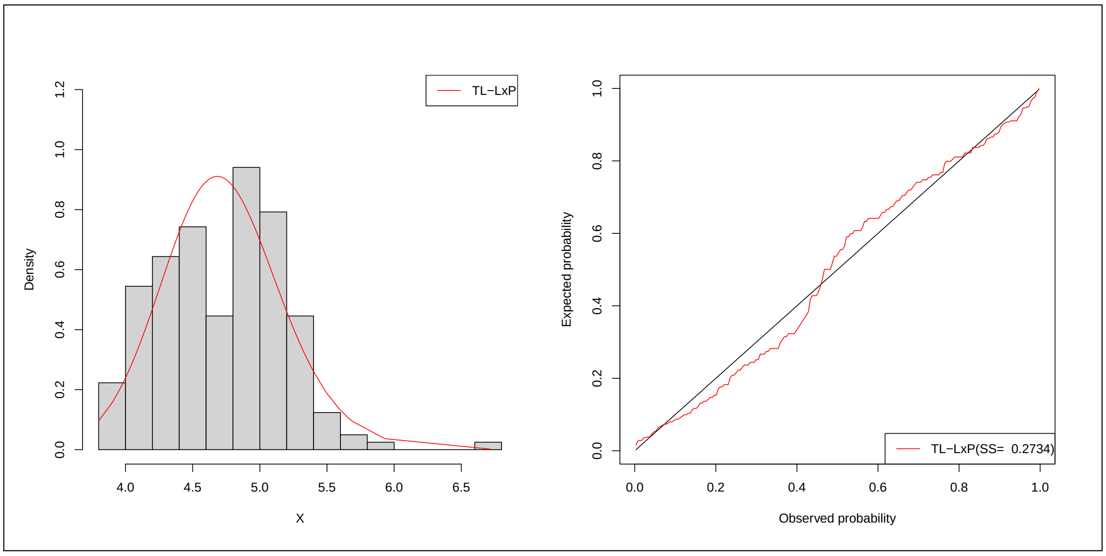

Figure 5. Fitted Densities and Probability Plots for Red Cells Count Data.

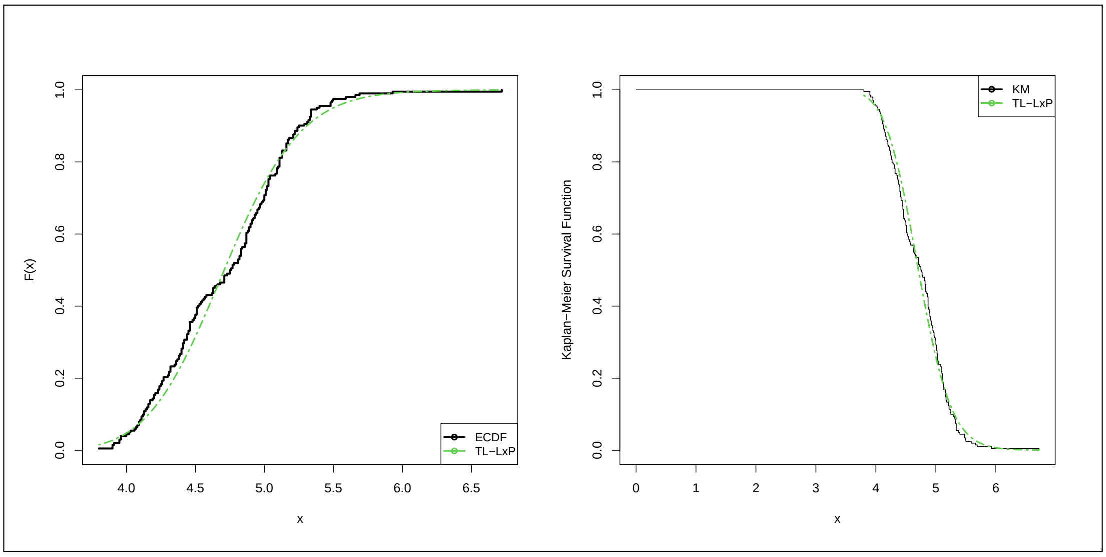

Figure 6. Fitted K-M and ECDF Plots for Red Cells Data.

 doi:10.20944/preprints202410.0885.v1

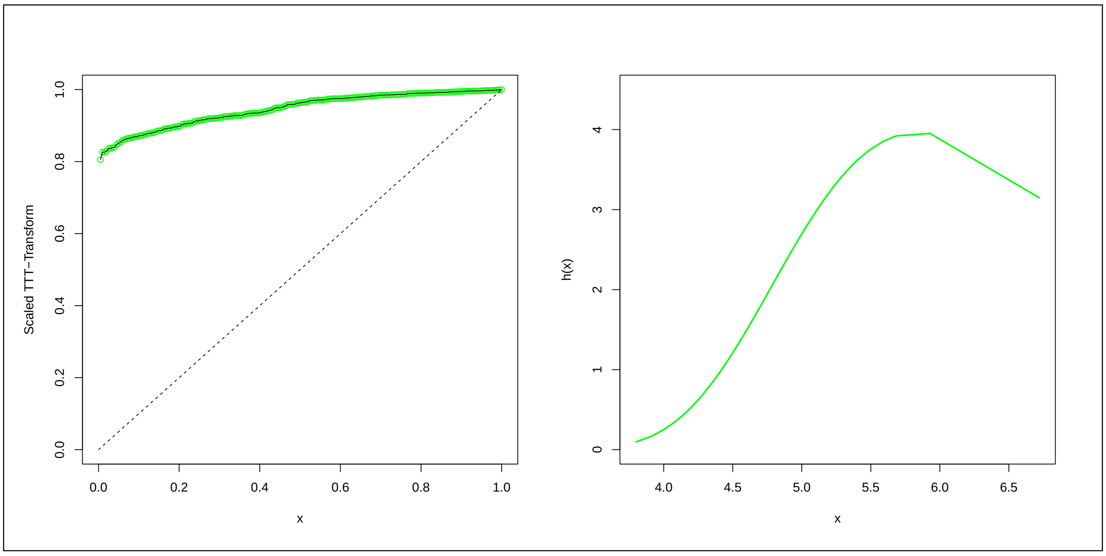

Figure 7. Fitted TTT and HRF Plots for Red Cells Data.

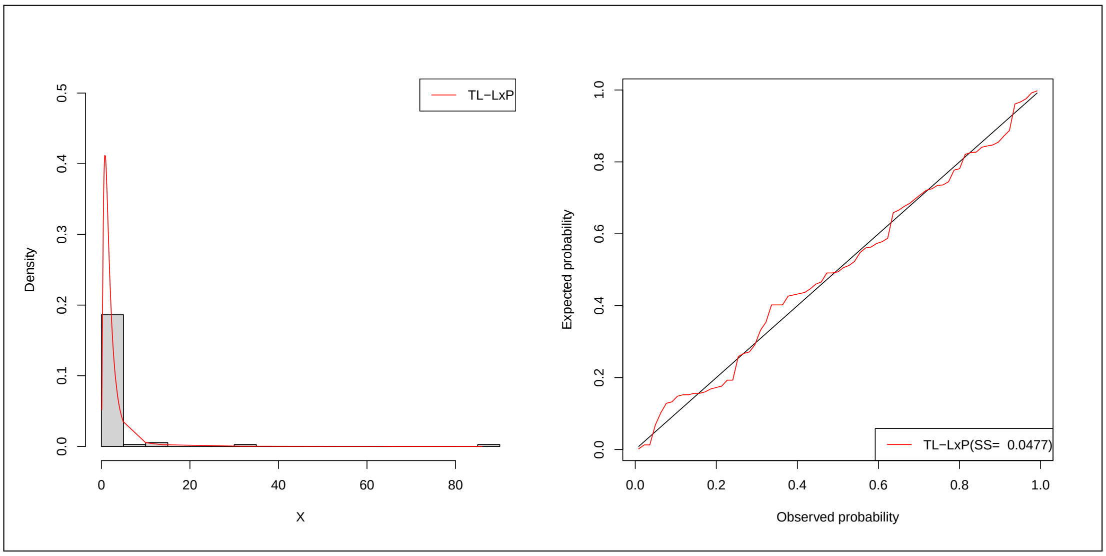

Figure 8. Fitted Densities and Probability Plots for Acute Bone Cancer Data.

The estimated variance-covariance matrix for the TL-LxP model for acute bone cancer dataset is given by

$$\begin{pmatrix} 0.5494 & -0.0559 & 0.2477 & -0.1902 \\ -0.0559 & 0.0978 & -0.0999 & -0.4936 \\ 0.2477 & -0.0999 & 0.1845 & 0.2232 \\ -0.1902 & -0.4936 & 0.2232 & 4.1950 \end{pmatrix}$$

and the approximate 95% two-sided confidence intervals for the parameter estimates are α, b, λ and θ are given by 2.5917 ± 1.4528, 0.5558 ± 0.6130, 0.5351 ± 0.8418 and 4.1833 ± 4.0144, respectively.

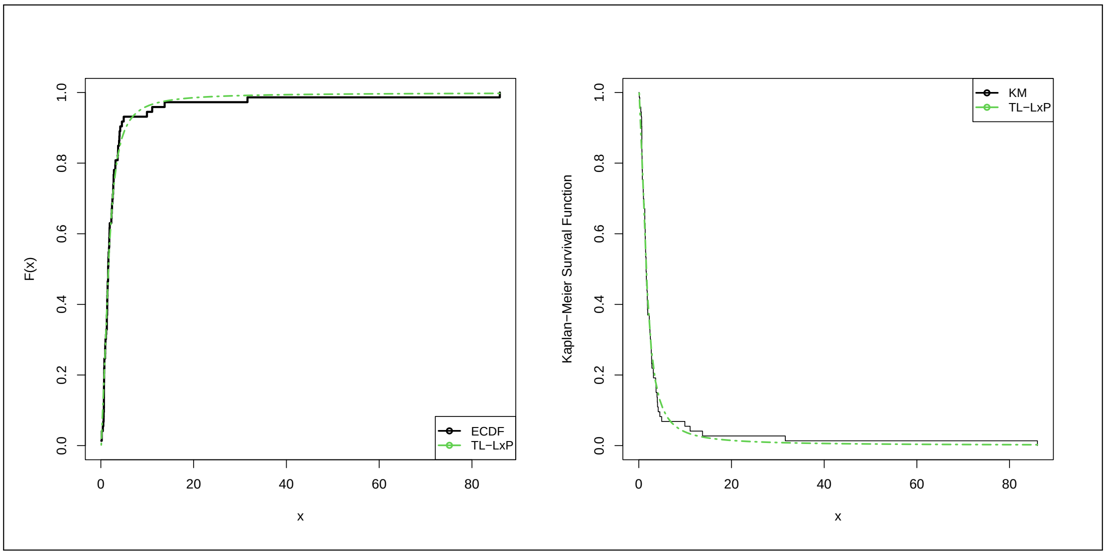

Figure 9. Fitted K-M and ECDF Plots for Acute Bone Cancer Data.

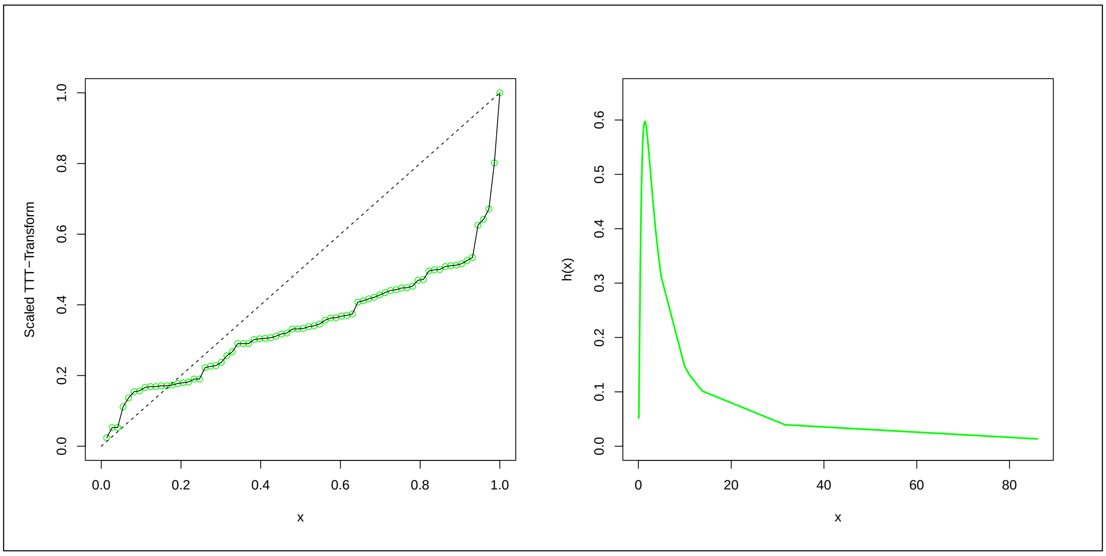

Figure 10. Fitted TTT and HRF Plots for Acute Bone Cancer Data.

7. Concluding Remarks

A new compounded distribution was developed. The new distribution is a generalization of the Lomax distribution via the Topp-Leone generalization and compounding using the Poisson distribution. Statistical properties for this distribution were derived. Results from applications to real datasets of the new model shows the utility of the proposed model in comparison to some selected models.

References

1. Aarset, M. V. (1987). How to Identify Bathtub Hazard Rate. IEEE Transaction of Reliability, 36(1), 106-108.
2. Abdul-Moniem, I. B. and Abdel-Hameed, H. F. (2012). On Eponentiated Lomax Distribution. International Journal of Mathematical Archive, 3(5), 1-7.
3. Al-Shomrani, A., Arif, O., Shawky, A., Hanif, S., Shahbaz, M.Q. (2016). The Topp-Leone Family of Distributions: Some Properties and Application. Pakistan Journal of Statistics and Operation Research, 12(3), 443-451.
4. Alzaatreh, A., Lee, C. and Famoye, F. (2013). A New Method for Generating Families of Continuous Distributions. Metron, 71(1), 63-79.

5. Bassiouny, A. H., Abdo, N. F., and Shahen, H. S. (2015). Exponential Lomax Distribution. Journal of Computer Applications, 121(13), 24-29.
6. Chipepa, F. and Oluyede, B. (2021). The Topp-Leone Odd Exponential Half Logistic-G Family of Distributions with Applications. Pakistan Journal of Statistics, 37(3), 253–277.
7. Cordeiro, G. M., Alizadeh, M., Ortega, E. M., (2014). The Exponentiated Half-Logistic Family of Distributions: Properties and Applications. Hindawi Publishing Corporation Journal of Probability and Statistics Volume 2014, Article ID 864396, 21 pages. DOI: 10.1155/2014/864396
8. Johnson, N. L., Kotz, S., and Balakrishnan, N. (1994). Continuous Distributions, Volume 1, John Wiley & Sons, New York, NY.
9. Lomax, K.S. (1954). Business Failures: Another example of the Analysis of Failure Data. Journal of the American Statistical Association 49, 847-852.
10. Mansour, M., Yousof, H.M., Shehata, W.A., and Ibrahim, M.(2020). A New two Parameter Burr XII Distribution: Properties, Copula, Different Estimation Methods and Modeling Acute Bone Cancer Data. Journal of Nonlinear Science and Applications, 13, 223-238.
11. Moakofi, T., Oluyede, B. and Gabanakgosi, M. (2022). The Topp-Leone Odd Burr III-G Family of Distributions: Model, Properties and Applications. Statistics Optimization and Information Computing, 1, 1–27.
12. Oluyede, B., Dingalo, N. and Chipepa, F. (2023). The Topp-Leone-Harris-G Family of Distributions with Applications. International Journal Mathematics in Operational Research, 24(4), 554-582.
13. Oguntunde, P. E., Khaleel, M. A., Okbue, H. I., and Odetunmibi, O. A. (2019). The Topp-Leone Lomax Distribution with Applications to Airborne Communication Transceiver Dataset. Wireless Personal Communications, 109, 349-360.
14. Rényi, A. (1960). On Measures of Entropy and Information. Proceedings of the Fourth Berkeley Symposium on Mathematical Statistics and Probability, 1, 547 - 561.
15. Ristić, M. M. and Balakrisihnan, N. (2012). The Gamma Exponentiated Exponential Distribution. Journal of Computation and Simulation, 82, 1191-1206.
16. Shannon, C. E. (1951). Prediction and Entropy of Printed English, The Bell System Technical Journal, 30, 50-64.
17. Tahir, M. H., Cordeiro, G. M., Mansoor, M., and Zubair, M. (2015). The Weibull-Lomax Distribution: Properties and Applications. Hacettepe Journal of Mathematics and Statistics, 44(2), 455-474.
18. Torabi, H. and Montazari, H. N. (2012). The Gamma-Uniform Distribution and its Applications. Kybernetika, 48(1), 16–30.
19. Weibull W. A. (1951). Statistical Distribution Function of Wide Applicability. Journal of Applied Mechanics, 18, 293-296.
20. Zografos, K. and Balakrishnan, N. (2009). On Families of Beta- and Generalized Gamma Generated Distributions and Associated Inference. Statistical Methodology, 6, 344-362.